GPS Signal Multipath
A Software Simulator

Sung H. Byun, George A. Hajj, and Lawrence E. Young Jet Propulsion Laboratory

Simulation is a key activity in almost all areas of science and engineering. It enables researchers and developers to characterize a system's performance before it is built or deployed. In fact, simulation studies can help at the system design stage to maximize the future system's performance. In last month's column, we focused on the simulation of different scenarios under which a global navigation satellite system receiver might operate, accounting for such operating parameters as receiver measurement precision and satellite visibility. We now turn to the simulation of the phenomenon of multipath and its effect on GPS observables. A team of researchers at the California Institute of Technology's Jet Propulsion Laboratory (JPL) has developed a multipath simulator which is being used to optimize the choice and location of a GPS antenna to be placed on the International Space Station's Japanese Experiment Module. The antenna will feed a GPS receiver which will help to assess the accuracy of an atomic clock to be flown on the space station. The receiver will be used to determine the position and velocity of the space station with sufficient accuracy to correct the clock's measurements for the effects of special and general relativity.

In this month's column, Sung Byun, George Hajj, and Larry Young discuss the operation of their simulator and some of the results they have obtained for the space station environment. Sung Byun received his Ph.D. degree in aerospace engineering and engineering mechanics from the University of Texas at Austin. He is currently working in the Tracking Systems and Applications Section at JPL. His main research is focused on low Earth orbiter (LEO) trajectory determination using GPS and on other scientific applications of GPS. George Hajj received his Ph.D. in physics from Rice University. He is a principal member of the technical staff at JPL. His research interests include the use of GPS-LEO occultations for remote sensing of the Earth's atmosphere, ionospheric tomography, and ionospheric data assimilation. Larry Young received his Ph.D. in nuclear physics from the State University of New York at Stony Brook. He has developed radiometric technology at JPL since 1978, currently supervising a group developing high precision GPS receiver applications. He served on the National Research Council's 1995 Committee on the Future of GPS, and is currently (2000/2002) Space Representative on The Institute of Navigation's council.

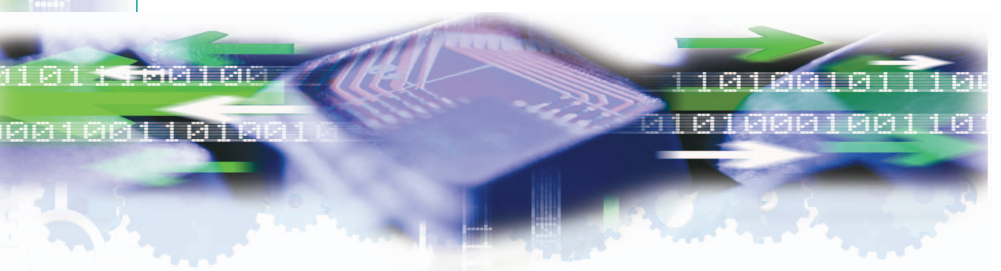

Researchers and developers around the world have shown that the Global Positioning System is capable of supporting a huge variety of applications with different levels of required accuracy and availability. At the high-accuracy end of the application spectrum, relative position (baseline) solution accuracies using GPS are 1-2 parts in 10^9, while those of orbit positioning are larger by only a couple of parts in 10^9. A wide range of techniques have been developed over the past two decades which allow GPS users to achieve such accuracies. Data accuracies are limited by instrumental thermal noise, tropospheric effects, higher order ionospheric effects, and multipath. Instrumental noise in advanced receivers is now reaching a root-mean-square (r.m.s.) level of 10 centimeters for range (P-code) and 0.1 millimeter for range-rate (phase) after one second averaging. The tropospheric effect can be modeled to the centimeter-level while higher-order ionospheric effects, under normal conditions, are expected to be less than 1 centimeter or so.

Differential GPS can greatly reduce common-mode errors resulting from atmospheric delay, GPS orbit, and satellite and/or receiver clocks. However, the GPS multipath errors cannot be removed by the differential approach since multipath is a highly localized phenomenon. Thus, one of the major potential error contributors to GPS positioning applications is multipath.

Multipath is the phenomenon in which a signal arrives at an antenna via several paths due to signal reflection and diffraction. Multipath error is scaled according to wavelength and is generally therefore nearly 100 times larger for P-code pseudoranges than it is for carrier-phase measurements. Instantaneous multipath error can be as large as a few meters for P-code and a few centimeters for carrier phase. Thus, in situations in which instantaneous range and phase data are needed, multipath becomes a dominant source of error in the measurement.

At the Jet Propulsion Laboratory, we are examining the effect of multipath on GPS signals and its implications on orbit and ground positioning with the aid of a multipath simulator known as MUSTARD (MUltipath Simulator Taking into Account Reflection and Diffraction). In this article, we will describe the theoretical background of multipath and the applications we have studied using the simulator.

Multipath Problem. If a satellite's signal propagates along a direct path to the receiver's antenna, the receiver can accurately determine the satellite's range. However, the GPS signal can be easily reflected by nearby objects, thus resulting in possible multiple secondary paths as shown in **Figure 1**. These paths are always longer than the direct path, and are superimposed on the direct signal at the antenna with a different phase and amplitude. The signal waveform's amplitude and phase can be significantly distorted by these secondary paths and thus can result in significant ranging errors.

Multipath Simulator. Previous multipath research has focused mostly on mitigating multipath errors. However, in the early design phase of an experiment, it would be desirable to predict hazardous environmental configurations which can cause severe multipath. With this information, we may attempt to modify the structural configuration if possible, or recommend the best antenna type, location, and orientation within the given configuration. The multipath simulator, MUSTARD, is a valuable tool for this kind of study.

In essence, the simulator traces the signal as it is transmitted by the GPS satellite to a user's receiver accounting for all possible paths the signal can take by reflecting or diffracting off the surrounding surfaces. We have modeled reflection and diffraction using the Uniform Geometrical Theory of Diffraction.

The use of this theory (rather than physical optics) sets a lower limit of a few wavelengths on the size of the reflecting objects which can be considered. (In the case of GPS, this means a limiting dimension of not much less than about one meter.) The multipath signals are added to the direct signal after accounting for the gain of the receiving antenna. The software then simulates the receiver's tracking loop and estimates pseudorange and carrier-phase multipath error. This is done for both GPS frequencies.

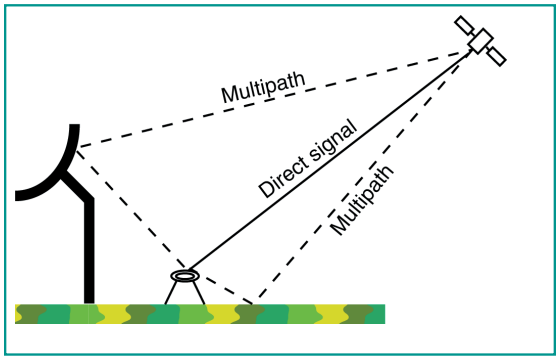

FIGURE 1 A multipath generating environment

This multipath simulator gives a realistic estimate of the error introduced by multipath and helps to find a means of minimizing its effect. For precise orbit determination, for example, it provides a quantitative estimate of multipath errors and, thus, can be used for testing different ways of processing simulated observables containing multipath errors.

GPS Signal Structure

A GPS satellite transmits two right-hand circularly polarized (RCP) signals at L-band frequencies: L1 at 1575.42 MHz and L2 at 1227.6 MHz. The L2 signal and the in-phase component of the L1 signal are modulated by a pseudorandom precision code (P-code) at a frequency of 10.23 MHz; the quadrature component of L1 is modulated by a coarse acquisition (C/A) code at a frequency of 1.023 MHz. A suitably equipped receiver will determine amplitude, pseudorange, and carrier-phase measurements for each of the C/A, L1 P-code (P1), and L2 P-code (P2) signals.

Because the characteristics of C/A and P1 multipath errors are very similar, our discussion below is simplified by considering only one of the two signals. Differences between P1 and C/A multipath will be pointed out as they become significant. To that end, it is convenient to model the transmitted P1 and P2 signals as the real part of

$$S_i(t_T) = \tilde{A}_i P(t_T)\exp(j(\omega_i t_T + \phi_{Ti}))$$

where

t_T = transmission time (on satellite time scale)

i = index for L1 and L2, respectively

$\tilde{A}_i$ = signal amplitude

P = PRN code

$\omega_i = 2\pi f_i$, where f_i is the transmitted frequency

ϕ_{Ti} = transmitter bias between carrier and P-code.

The equation does not show the Y (encrypted) code, the C/A-code component on L1, or the data modulation at 50 bits per second. Note that the transmitter oscillator drift term is included in t_T.

Due to the dispersive nature of the ionosphere, the L1 and L2 signals travel at different velocities. Moreover, the group and phase velocities are different for each frequency. Therefore, we can write the received signal as:

$$R_i(t_R) = A_i P(t_R - \tau_i^g)\exp\left(j(\omega_i(t_R - \tau_i^p) + \phi_{Ri})\right)$$

where the additional terms are

t_R = reception time (on receiver time scale)

A_i = the received signal amplitude

τ_i^g = pseudorange

τ_i^p = τ_i^g + differential ionospheric effect on phase

ϕ_{Ri} = ϕ_{Ti} + bias between carrier and P-code.

Note that t_R includes the receiver oscillator drift term. Both τ_i^g and τ_i^p include the transmitter and receiver clock biases. A single GPS measurement consists of four observables: two phase measurements, one for the L1 frequency and one for the L2 frequency,

$$\Phi_i = -\omega_i \tau_i^p + \phi_{Ri}$$

with an unknown bias, and two pseudorange measurements,

$$P_i = c\,\tau_i^g$$

By ignoring terms of order $1/f_i^3$ or higher, these observables can be written in units of distance as:

$$L_1 \equiv -c\frac{\Phi_1}{2\pi f_1} = \rho + n_1\lambda_1 - \frac{q}{f_1^2} + M_{L1}$$

$$L_2 \equiv -c\frac{\Phi_2}{2\pi f_2} = \rho + n_2\lambda_2 - \frac{q}{f_2^2} + M_{L2}$$

$$P_1 = \rho + \frac{q}{f_1^2} + M_{P1}$$

$$P_2 = \rho + \frac{q}{f_2^2} + M_{P2}$$

where ρ is the non-dispersive delay including the geometric delay, tropospheric delay, clock biases, and any other delay that effects all observables similarly; q is a parameter which is proportional to the ionospheric total electron content (TEC), which is the integrated electron density between the transmitter and the receiver. Other parameters are:

c = the speed of light

λ_i = the wavelength for L1 and L2

n_i = unknown number of integer cycles

q/f_i^2 = ionospheric group delay and phase advance

M_{Li} = carrier multipath

M_{Pi} = code multipath.

Terms which contribute to the observables but are not included in the above equations are data noise, phase center variation, higher order ionospheric terms, and a "wind-up" transmitter-receiver geometry-dependent term. We will assume these terms to be negligible. Alternatively, they can be modeled and subtracted out.

Of importance to the subsequent analysis are the ionosphere-free linear combinations:

$$PC = \left(\frac{f_1^2}{f_1^2 - f_2^2}\right)P_1 - \left(\frac{f_2^2}{f_1^2 - f_2^2}\right)P_2$$

$$= \rho + \left(\frac{f_1^2}{f_1^2 - f_2^2}\right)M_{P1} - \left(\frac{f_2^2}{f_1^2 - f_2^2}\right)M_{P2}$$

$$LC = \left(\frac{f_1^2}{f_1^2 - f_2^2}\right)L_1 - \left(\frac{f_2^2}{f_1^2 - f_2^2}\right)L_2$$

$$= \rho + \frac{f_1^2 M_{L1} - f_2^2 M_{L2}}{f_1^2 - f_2^2} + \frac{f_1^2 n_1\lambda_1 - f_2^2 n_2\lambda_2}{f_1^2 - f_2^2}$$

In the above equations, the ionospheric term is removed and one is left with the pseudorange or biased carrier-phase plus a linear combination of L1 and L2 multipath. For the GPS L1 and L2 frequen-

cies, the coefficients multiplying P1 and P2 in the above equation are 2.54... and −1.54... respectively. This implies that, if P1 and P2 multipath errors are about equal but uncorrelated, the multipath peak-to-peak amplitude is magnified by about a factor of 3 compared to that of either P1 and P2 alone. A similar analysis applies for the carrier-phase linear combination equation.

Multipath Effect

Since the multipath error for GPS pseudorange observables is much larger than that for carrier phase, we will concentrate more on the effects of multipath on GPS code measurements. In order to understand the effects of multipath in any given environment, we need to understand how code-correlating receivers operate and how multipath distortion results in ranging errors. The receiver's response to multipath can be parameterized by signal amplitude, time delay, phase, and phase rate. Note that all of the parameter values are relative to the direct GPS signal.

In tracking the GPS code signal, the received signal is correlated with a locally generated replica of the code. A conventional receiver typically computes the correlation function between the received signal and the internally-generated signal at three different modeled delays called "prompt", "early", and "late". The "early" and "late" delays differ from the "prompt" delay by plus and minus the receiver sampling interval, $+S$ and $-S$ nanoseconds, respectively. The receiver effectively fits an equilateral triangle with base length equal to twice the code chipping period, $2T$, on these three points and declares the location of the peak to be the true delay. In the absence of any multipath, the correlation between the received signal and the receiver-generated code can be approximated by an equilateral triangle with a peak value of A and a phase $(\phi_m - \phi)$ where ϕ_m is the modeled phase. In the presence of a single multipath signal with an additional time delay $\Delta\tau_1$, amplitude A_1, and phase shift ϕ_1, the correlation function can be modeled as the sum of the two triangles corresponding to the direct signal and to the multipath signal. The presence of multipath signals corrupts the triangular shape and shifts the peak, thereby introducing an error in the delay measurement. As the satellite elevation angle changes, the size of the error will increase to a maximum and then decrease, swing negative and then back to positive again and so on, in a quasi-cyclical manner.

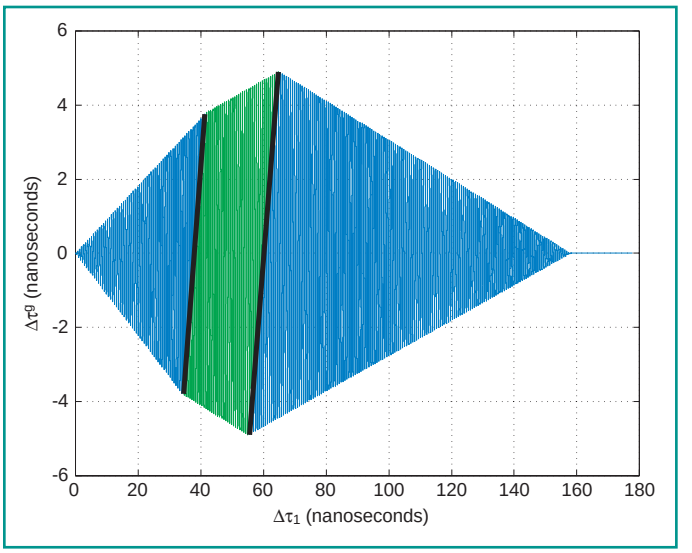

FIGURE 2 The P1 code tracking error when $S > T/2$ as a function of a single multipath source with multipath delay of $\Delta\tau_1$. The relative multipath amplitude is assumed constant ($A_1/A = 0.1$); values of $T = 98$ nanoseconds and $S = 60$ nanoseconds were used. Regions 1–3 are separated by thick solid lines for clarity. A delay of 100 nanoseconds corresponds to an additional path length of about 30 meters.

A receiver's response to a multipath-contaminated signal depends on the relationship between the receiver sampling interval and the code-chip length. We can consider two main receiver categories: wide-sampling receivers where $S > T/2$ and narrow-sampling receivers where $S < T/2$.

Wide Sampling Interval. In the case of sampling intervals longer than half of the chip length, the resulting error in the code measurement, $\Delta\tau^g$, induced by the presence of a single multipath component with delay, $\Delta\tau_1$, can be categorized by four different regions:

Region 1: $\Delta\tau_1 < T - S + \Delta\tau^g$
Region 2: $T - S + \Delta\tau^g < \Delta\tau_1 < S + \Delta\tau^g$
Region 3: $S + \Delta\tau^g < \Delta\tau_1 < T + S + \Delta\tau^g$
Region 4: $\Delta\tau_1 > T + S$: no mulipath error.

Figure 2 shows the P1 pseudorange multipath induced error, $\Delta\tau^g$, as a function of the multipath delay, $\Delta\tau_1$. The envelope of the multipath error can be readily seen in the figure. The upper envelope corresponds to the multipath error which is in phase with the direct signal, while the lower envelope corresponds to the out-of-phase case. The three different slopes of the upper and lower envelopes correspond to the three different multipath regimes.

This figure also indicates that the amplitude changes asymmetrically for in-phase and out-of-phase multipath. The asymmetry of the envelope is amplified for higher values of the ratio A_1/A. This implies that multipath does not average out but introduces a bias when integrated over a complete cycle of multipath error. This could cause a significant bias when A_1/A is not small.

The C/A-code pseudorange multipath-induced error can also be categorized by the same four regions as long as $S > T/2$, where T is the C/A-code chipping period. This causes the different regimes to trigger at different values of $\Delta\tau_1$ compared to the P-code. Specifically, the C/A-code multipath-induced error can grow to be 10 times larger than the P-code error and does not vanish until $\Delta\tau_1 > T + S$. On the other hand, for various reasons, it is the region of small multipath delays that is of greatest importance for most GPS applications, and in this region the P1 and C/A-code multipath errors are the same.

Narrow Sampling Interval. When $S < T/2$, $\Delta\tau^g$ is categorized by four different regions:

Region 1: $\Delta\tau_1 < S + \Delta\tau^g$
Region 2: $S + \Delta\tau^g < \Delta\tau_1 < T - S + \Delta\tau^g$
Region 3: $T - S + \Delta\tau^g < \Delta\tau_1 < T + S$
Region 4: $\Delta\tau_1 > T + S$: no multipath error.

Note that the boundary values of each region are different from those of the wide-sampling case. A main distinction between the narrow and wide sampling interval cases is that in the former, the error exhibits a constant peak value in region 2 as shown in Figure 3. Note that the C/A-code multipath-induced error exhibits a very wide region 2 and does not vanish until $T + S = 1028$ nanoseconds (the C/A-code chip width).

When $A_1/A << 1$, region 1 translates to $\Delta\tau_1 < T - S$ (wide sampling) and to $\Delta\tau_1 < S$ (narrow sampling). For S equal to 60 nanoseconds (wide sampling) and 48 nanoseconds (narrow sampling), this trans-

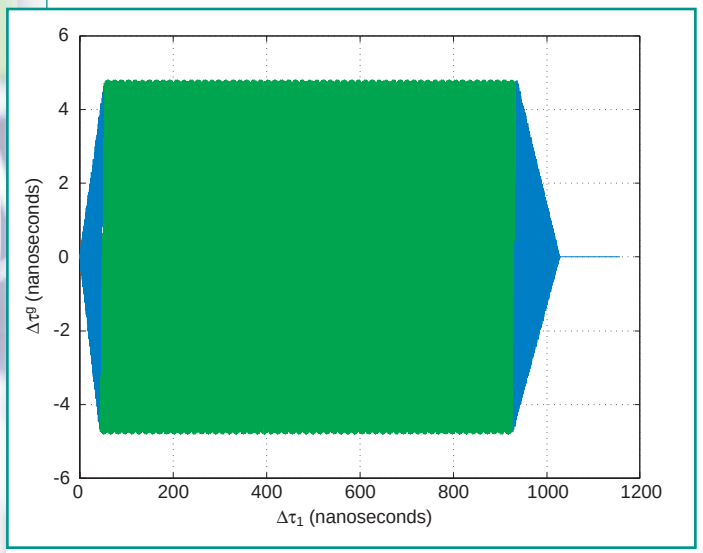

FIGURE 3 The C/A-code tracking error when $S < T/2$ as a function of $\Delta\tau_1$. Values of $A_1/A = 0.1$, $T = 980$ nanoseconds, and $S = 48$ nanoseconds have been used.

lates to $c\Delta\tau^g < 11$ meters and $c\Delta\tau^g < 14$ meters, respectively. These values are larger than the multipath distances with which we will deal in our discussion later.

Simulator Description

At JPL, we have developed MUSTARD for analyzing the effects of GPS signal multipath. This software uses a ray-tracing technique to determine the different paths that a GPS transmitted signal can take. The capabilities of the simulator include:

- GPS signals: Handles both L1 and L2 frequencies; simulates RCP and LCP reflected and diffracted signals; estimates the multipath delay in the pseudorange and carrier-phase measurements.
- Reflection modeling: Uses the Uniform Geometrical Theory of Diffraction to model signal reflection and diffraction from surfaces, edges, and corners; handles simultaneous reflections from many surfaces.
- Antenna and receiver: Simulates the antenna gain pattern for RCP and LCP signals for L1 and L2; simulates a receiver's operations on incoming signals which produce output observables.
- Surrounding environment modeling: Models flat surfaces of arbitrary shape, spheres or sections of spheres (antenna dishes, inside and outside surfaces), cylinders or sections of cylinders, conducting or dielectric surfaces.
- Geometry: Models the motion of the GPS satellites and receivers and their attitudes to derive time series of the multipath error.

Modeling the multipath effects can help determine optimum configurations of the surrounding environment as well as predict the errors that the system will experience. Therefore, this software is especially useful in the design phase of a flight mission or of ground experiments to quantify the effect of the signal multipath for different GPS antenna types and locations.

Multipath Modeling. The simulator uses a simplified model of the real multipath environment where the geometry of the reflecting structures and the transmitting and the receiving antennas are approximated. The multipath environment is generally modeled as a finite number of surfaces whose dimensions, relative locations, and orientations, as well as their electromagnetic properties are specified.

As mentioned above, in modeling the reflection and diffraction from each surface, the Uniform Geometrical Theory of Diffraction is used. The details of this theory have been worked out for many types of surfaces with different shapes and electromagnetic properties.

Antenna Gain Pattern. Partial multipath signal rejection can be achieved by properly shaping the antenna gain pattern for both polarizations. Usually,

Terminology

Polarization. The electric field that describes the wave propagation is a vector which lies in a plane perpendicular to the direction of propagation. If we consider that the electric field has two orthogonal components in this plane (E_x and E_y), then the phase differences between them determine the kind of polarization the wave has. If they are in phase, the wave is plane-polarized (the end of the electric field vector oscillates in a straight line); if they are not in phase, the wave has an elliptical polarization (the end of the electric field vector moves around in an ellipse).

Circular Polarization. A special case of elliptical polarization where the end of the electric field vector travels around a circle. This happens when the phase difference between E_x and E_y is 90 degrees.

Right-hand Circular Polarization (RCP). Circular polarization with the end of the electric field vector going around in a counterclockwise direction when we look at it as the wave comes straight toward us.

Left-hand Circular Polarization (LCP). Circular polarization with the end of the electric field vector going around in a clockwise direction when we look at it as the wave comes straight toward us.

Maxwell's Equations. These equations bear the same relationship to electromagnetism that Newton's laws of motion do to mechanics. Basically, they describe the behavior of an electric field, a magnetic field, an electric field produced by a changing magnetic field, and a magnetic field produced by a changing electric field as they vary in time and in space.

Diffraction. Diffracted rays are produced by incident rays which hit edges, corners, or vertices of boundary surfaces. An incident electromagnetic wave is divided at the obstruction into many infinitesimal wavelets which then interfere with each other as they proceed.

Reflection. A process affecting an electromagnetic wave where a medium discontinuity (say between air and a metal surface) turns back a portion of the incident radiation into the medium through which the radiation approached.

Geometrical Optics. In situations where the wavelengths involved are very small compared with the dimensions of interacting objects, we can make a rough first approximation of Maxwell's equations to characterize the behavior of electromagnetic waves. This approach is valid as long as the waves do not encounter obstacles comparable in size to the wavelength of the radiation. Geometrical optics is often used to determine the distribution of light intensity, polarization, and wave phase throughout space.

Geometrical Theory of Diffraction (GTD). An extension of geometrical optics which accounts for diffraction. It introduces diffracted rays by means of several laws of diffraction which are analogous to the laws of reflection and refraction.

Uniform Geometrical Theory of Diffraction. An extension of GTD in transition regions adjacent to shadow and reflection boundaries, where the diffraction coefficient of the original GTD is not precise.

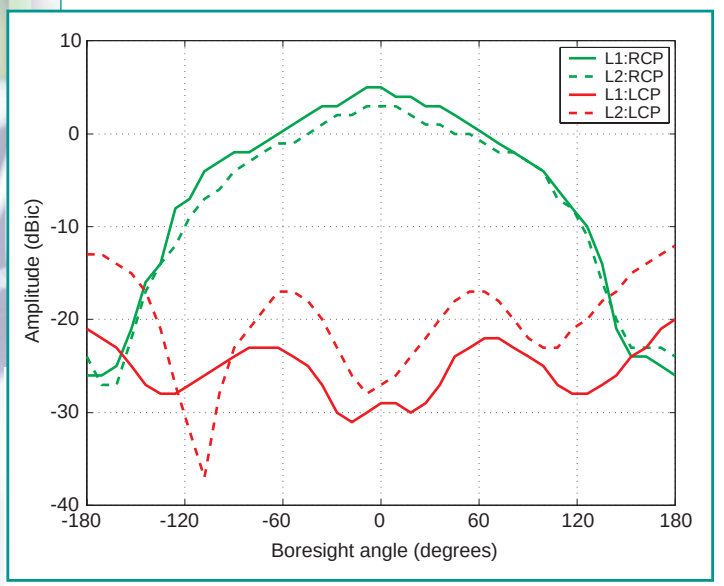

FIGURE 4 The gain pattern of a Dorne-Margolin antenna. Note that 0° corresponds to the antenna boresight direction.

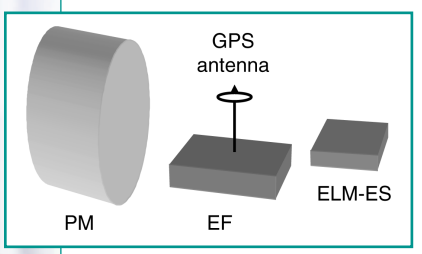

FIGURE 5 The environmental modeling of reflecting surfaces of the Japanese Experiment Module showing the Pressurized Module (PM), Exposed Facility (EF), and Experiment Logistic Module-Exposed Section (ELM-ES).

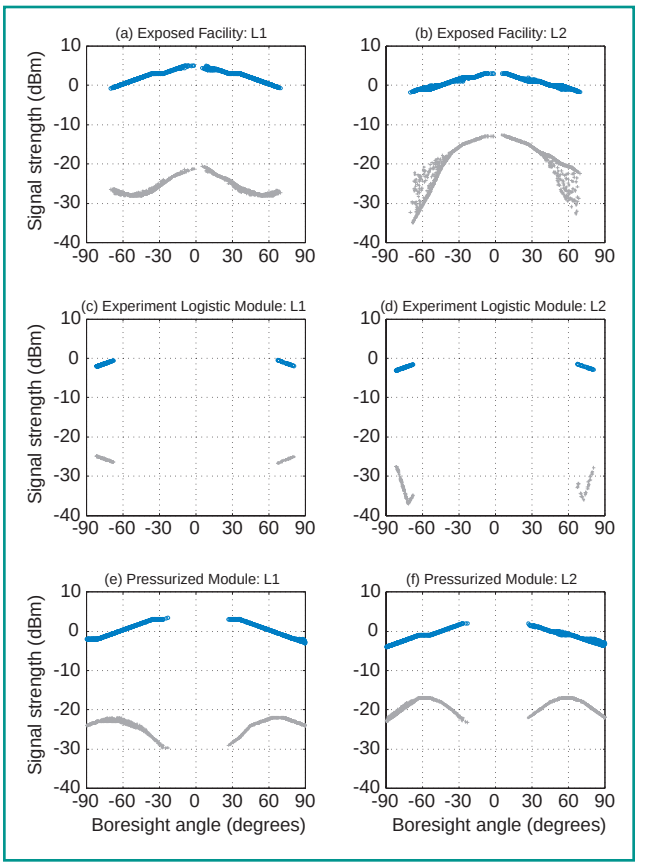

FIGURE 6 A comparison of the direct (blue) and specular reflected (gray) signal strength for the EF, ELM-ES, and PM structures.

the antenna gain pattern is shaped in such a way that overall gain, and particularly LCP gain, drop off quickly at low elevation angles so that reflected signals received at very low and negative elevation angles are significantly attenuated. Signals from low elevation angles are more likely to be reflected from a nearby object.

Figure 4 shows an example of a GPS receiving antenna gain pattern corresponding to a Dorne-Margolin (D-M) antenna (a modified drooping crossed dipole with no additional back plane). The figure depicts the antenna gain as a function of boresight angle for a specific azimuthal angle and for L1, L2, RCP, and LCP. The multipath simulator can accommodate any particular antenna gain pattern.

Application of the Simulator

Using the MUSTARD GPS multipath simulator, we can carry out various tests in an attempt to reduce the multipath effects. For example, we can try to find the optimal GPS antenna location and attitude, select the best antenna gain pattern, or try different data analysis schemes to improve the overall parameter solution obtained from the GPS data.

MUSTARD has been used in the early design phase of several satellite missions operated by JPL. Recently, the simulator was used to study the Primary Atomic Reference Clock in Space (PARCS) experiment. The purpose of PARCS is to demonstrate state-of-the-art atomic clock performance in space. The microgravity environment of space allows significant improvements in clock performance over ground-based clocks, thus opening up potential ultra-precise reference clocks in space. The demonstration will be carried out on the International Space Station (ISS). It will carry a laser-cooled precision clock driven by a hydrogen maser. GPS measurements will accurately determine the ISS orbit. The orbit is needed for the precise determination of the ISS velocity and position in the Earth's gravitational field, in order to correct for the effects of special and general relativity on the PARCS clock behavior. The GPS antenna will be located on the Japanese Experiment Module (JEM) where the multipath interference will be severe.

Spacecraft Modeling. We modeled the ISS with a circular orbit at 407-kilometer altitude and used JPL's GIPSY/OASIS software to generate the nominal ISS orbit. We simulated the L1, L2, and ionosphere-free GPS pseudorange and carrier-phase data between the ISS and all visible GPS satellites over one day.

For modeling JEM's environment, we considered simplified models of three major multipath sources as shown in Figure 5 (roughly to scale). They are all stationary objects within about 10 meters of the GPS antenna.

Assessing the Multipath Error. For our study, we used the D-M antenna pattern shown in Figure 4, assuming azimuthal symmetry. We assumed the antenna to be placed at the center of the EF, but one meter above its top surface. We assumed the on-board GPS receiver tracks all visible GPS satellites, with an antenna elevation cutoff angle at 0°.

Figure 6 shows relative strengths of the direct and reflected signals at L1 and L2 frequencies from each modeled surface. The horizontal axis of each plot indicates the angle of arrival of the direct signal

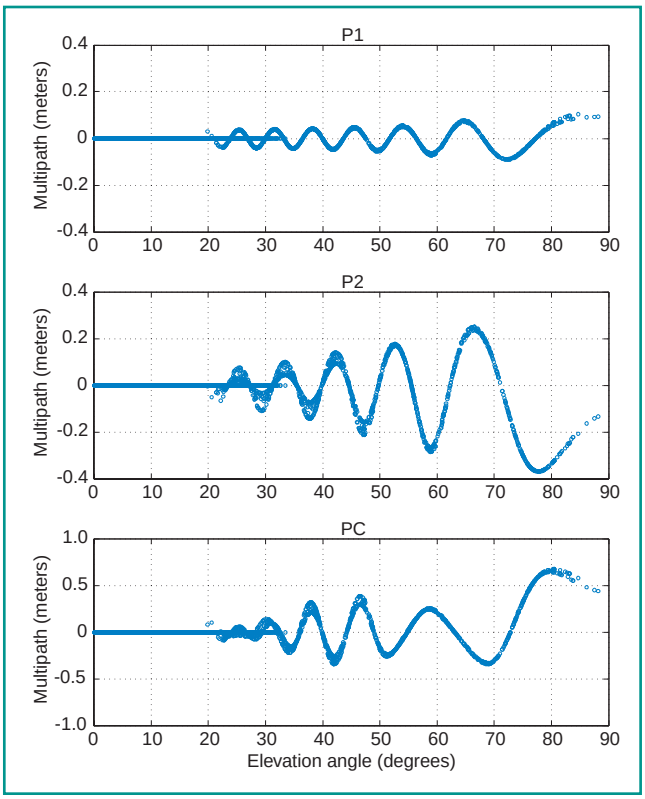

FIGURE 7 P-code multipath errors due to signal reflections from the EF as a function of the GPS satellite elevation angle. Multiple values correspond to different GPS satellites.

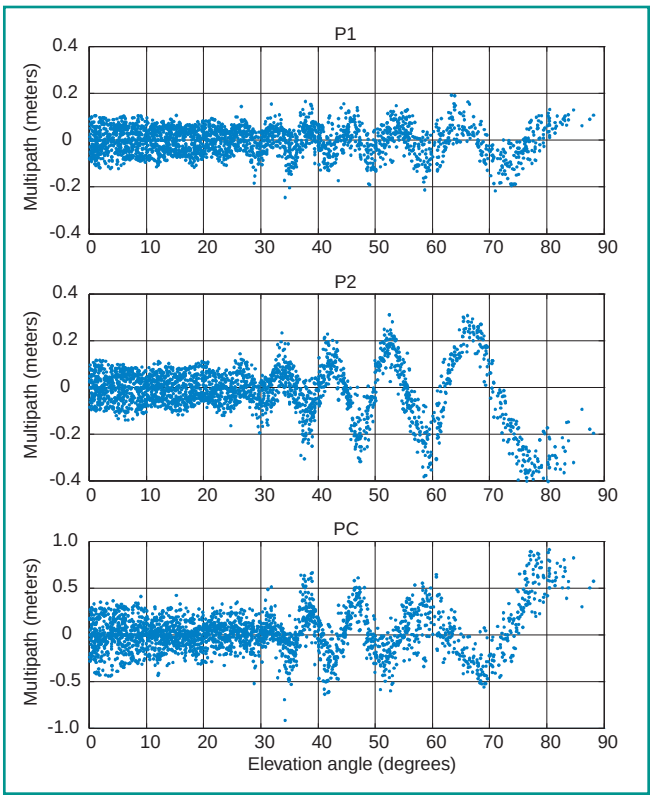

FIGURE 8 Same as Figure 7 but with diffraction included.

from a GPS satellite with respect to the antenna boresight. The blue points denote the direct signal strength while the gray points denote the reflected signal strength. In constructing these plots we considered only specular (smooth surface) reflection which explains the gaps at certain boresight angles. These gaps imply that no specular reflection is possible when the GPS satellite is within that boresight-angle range (the direct signal, although present, is not shown during these gaps). From this figure, we can see that the major multipath contributors are the EF and the PM but not the ELM. According to Figure 4, the antenna has better multipath attenuation characteristics at the L1 frequency (solid line) than at L2 (dotted line). Multipath attenuation is the separation between the RCP gain at the boresight angle (direct signal gain), and the LCP gain at 180° minus the boresight angle (reflected signal gain). This is also seen in Figure 6.

Figure 7 shows the P1, P2, and PC pseudorange multipath from the EF due to signal reflections only, from all visible GPS satellites as a function of the GPS satellite elevation angle. Plotting the multipath with respect to the elevation angle rather than time shows better the geometric characteristics of the reflecting structure. Such a representation can be beneficial in the early design phase of a spacecraft. The figure shows that multipath due to signal reflection from the EF is mainly from the satellites at high elevation angles. This is contrary to the general notion, but is explained by examining Figure 6 which shows the ratio of direct to multipath gain is greater toward the antenna boresight. Because of the worse L2-LCP antenna gain pattern relative to the L1-RCP (see Figure 4), the P2 signal has larger multipath errors than P1. PC has the highest multipath effect due to the multiplicative coefficients in the ionosphere-free linear combination equation.

Figure 8 shows the P1, P2, and PC pseudorange multipath from the EF due to both signal reflection and diffraction from all visible GPS satellites. Due to the small size of the EF, the signal diffraction from an edge at a low elevation angle can easily reach the antenna. By comparing Figures 7 and 8, it can be seen that the major multipath contribution is from signal diffraction at low elevation angles, and from signal reflection at high elevation angles. Even though not shown, very similar characteristics for carrier-phase multipath can be seen but at a scale 100 times smaller. Similar plots can be made for the P-code pseudorange multipath due to reflection and diffraction from the ELM and the PM. In total, the r.m.s. value of multipath is 0.71 meter for PC and 0.87 centimeter for LC.

Optimal Location of the Antenna. The effects of multipath on GPS measurements will depend on the antenna location with respect to the reflecting surfaces. When changing the surrounding environment is not an option, a simple approach to reducing multipath is to find the best antenna location within the restricted environment.

Since the purpose of this article is to illustrate the capability of MUSTARD, we have not performed an extensive search for the best antenna location on the JEM. Instead, the antenna location was fixed at the center of the EF, but its height was adjusted to illustrate the resulting multipath error variation. Table 1 shows the GPS antenna height effect on the multipath error. As the antenna is placed higher above the EF, the multipath errors are diminished. MUSTARD allows the user to choose a height which

satisfies a given orbit accuracy requirement. It is probable that better results could be obtained with a more easily accommodated flush-mounted antenna using a more favorably shaped antenna gain pattern.

Conclusion

In this article, we have briefly described our multipath simulator, MUSTARD. The simulator can be used in the initial design phase of an experiment to identify environmental configurations that can cause severe multipath. By using the simulator we can also determine the ideal antenna location, height, and orientation to minimize the multipath error within a given environment. Once the optimal geometric configuration is determined, MUSTARD can provide a realistic and quantitative estimate of multipath errors on GPS data. This in turn can provide a means of testing different ways of analyzing the data to minimize solution errors due to multipath. For a given environment, this simulator is a valuable tool for quantitatively assessing the multipath effect on GPS measurements.

TABLE 1 The GPS antenna height effect on multipath error (all values in meters).

Antenna height	PC	LC
0.2	0.7970	0.0108
1	0.7137	0.0087
2	0.7139	0.0077
3	0.7066	0.0070
4	0.6759	0.0067

Acknowledgments

This article is based on the paper "Development and Applications of a GPS Signal Multipath Simulator" to appear in the journal *Radio Science*. This research was carried out by the Jet Propulsion Laboratory, California Institute of Technology, under a contract with the National Aeronautics and Space Administration.

Further Reading

For further discussion on multipath, see

"Multipath Effects" by M.S. Braasch, Chapter 14 in *Global Positioning System: Theory and Applications*, Vol. I, edited by B.W. Parkinson and J.J. Spilker Jr., published by the American Institute of Aeronautics and Astronautics, Inc., Washington, D.C., 1996.

"Conquering Multipath: The GPS Accuracy Battle" by L.R. Weill in *GPS World*, Vol. 8, No. 4, April 1997, pp. 59–66.

Modelling and Simulation of GPS Multipath Propagation by B.M. Hannah, Ph.D. thesis, the Cooperative Research Centre for Satellite Systems, Queensland University of Technology, Brisbane, Australia, March 2001. An on-line version of the thesis is available at <http://adt.library.qut.edu.au/adt-qut/uploads/approved/adt-QUT20020326.160949/public/02whole.pdf>.

For more information on GPS antennas and antenna design, see

"A Primer on GPS Antennas" by R.B. Langley in *GPS World*, Vol. 9, No .7, July 1998, pp. 73-77.

"Characterizing the Behavior of Geodetic GPS Antennas" by B.R. Schupler and T.A. Clark in *GPS World*, Vol. 12, No. 2, February 2001, pp. 48-55.

Antenna Theory: Analysis and Design, 2nd ed. by C.A. Balanis published by John Wiley & Sons, New York, 1996.

For further information on GPS receiver operation in the presence of multipath, see

"Theory and Performance of Narrow Correlator Spacing in a GPS Receiver" by A.J. Van Dierendonck, P. Fenton, and T. Ford in *Navigation, the journal of The Institute of Navigation*, Vol.39, No.3, 1992, pp. 265–283.

For extended discussions of the geometrical theory of diffraction, see

Geometrical Theory of Diffraction for Electromagnetic Waves, 2nd ed. by G.L. James published by Peter Peregrinus Ltd., Stevenage, U.K. and New York, 1980.

"Geometrical Theory of Diffraction" by J.B. Keller in *Journal of the Optical Society of America*, Vol. 52, No. 2, February 1962, pp. 116–130.

"A Uniform Geometrical Theory of Diffraction for an Edge in a Perfectly Conducting Surface" by R.G. Kouyoumjian and P. Pathak in *Proceedings of the IEEE*, Vol. 62, No. 11, November 1974, pp. 1448–1461.

For discussions of multipath simulations for spacecraft missions, see

"Analysis of Orbit Errors Induced by Multipath for the ICESat Observatory" by P. Axelrad, K. Gold, P. Madhani, and A. Reichert in *Proceedings of ION GPS-99, the 12th International Technical Meeting of the Satellite Division of The Institute of Navigation*, Nashville, Tennessee, September 14-17, 1999, pp. 875-883.

"Frequency Transfer in Space with GPS Measurements" by S.C. Wu and S.H. Byun in *Proceedings of ION GPS-2001, the 14th International Technical Meeting of the Satellite Division of The Institute of Navigation*, Salt Lake City, Utah, September 11-14, 2001, pp. 2256-2262.

"Assessment of GPS Signal Multipath Interference" by S.H. Byun, G.A. Hajj, and L.E. Young in *Proceedings of The Institute of Navigation 2002 National Technical Meeting*, San Diego, California, January 28-30, 2002, pp. 694-705.

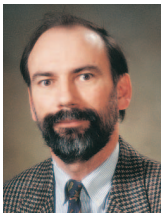

"Innovation" is a regular column featuring discussions about recent advances in GPS technology and its applications as well as the fundamentals of GPS positioning. The column is coordinated by Richard Langley of the Department of Geodesy and Geomatics Engineering at the University of New Brunswick, who appreciates receiving your comments as well as topic suggestions for future columns. To contact him, see the "Columnists" section on page 2 of this issue.